

## Temperature-dependent kinetic measurements and quasi-classical trajectory studies for the $\text{OH} + \text{H}_2/\text{D}_2 \rightarrow \text{H}_2\text{O} + \text{HDO} + \text{H/D}$ reactions

Oscar Martinez Jr., Shaun G. Ard, Anyang Li, Nicholas S. Shuman, Hua Guo, and Albert A. Viggiano

Citation: *The Journal of Chemical Physics* **143**, 114310 (2015); doi: 10.1063/1.4931109

View online: <http://dx.doi.org/10.1063/1.4931109>

View Table of Contents: <http://scitation.aip.org/content/aip/journal/jcp/143/11?ver=pdfcov>

Published by the AIP Publishing

### Articles you may be interested in

Low temperature rate coefficients of the  $\text{H} + \text{CH}^+ \rightarrow \text{C}^+ + \text{H}_2$  reaction: New potential energy surface and time-independent quantum scattering

*J. Chem. Phys.* **143**, 114304 (2015); 10.1063/1.4931103

A nine-dimensional ab initio global potential energy surface for the  $\text{H}_2\text{O} + \text{H}_2 \rightarrow \text{H}_3\text{O}^+ + \text{H}$  reaction

*J. Chem. Phys.* **140**, 224313 (2014); 10.1063/1.4881943

Dynamics of the  $\text{D}^+ + \text{H}_2 \rightarrow \text{HD} + \text{H}^+$  reaction at the low energy regime by means of a statistical quantum method

*J. Chem. Phys.* **139**, 054301 (2013); 10.1063/1.4816638

Nuclear spin dependence of the reaction of  $\text{H}_3^+$  with  $\text{H}_2$ . I. Kinetics and modeling

*J. Chem. Phys.* **134**, 194310 (2011); 10.1063/1.3587245

Cross sections of the  $\text{O} + \text{H}_2 \rightarrow \text{OH} + \text{H}$  ion-molecule reaction and isotopic variants ( $\text{D}_2$ , HD): Quasiclassical trajectory study and comparison with experiments

*J. Chem. Phys.* **123**, 174312 (2005); 10.1063/1.2098667



*APL Photonics* is pleased to announce  
Benjamin Eggleton as its Editor-in-Chief



# Temperature-dependent kinetic measurements and quasi-classical trajectory studies for the $\text{OH}^+ + \text{H}_2/\text{D}_2 \rightarrow \text{H}_2\text{O}^+/\text{HDO}^+ + \text{H/D}$ reactions

Oscar Martinez, Jr.,<sup>1</sup> Shaun G. Ard,<sup>1</sup> Anyang Li,<sup>2,a)</sup> Nicholas S. Shuman,<sup>1</sup> Hua Guo,<sup>2,b)</sup> and Albert A. Viggiano<sup>1,b)</sup>

<sup>1</sup>*Air Force Research Laboratory, Space Vehicles Directorate, Kirtland AFB, New Mexico 87117-5776, USA*

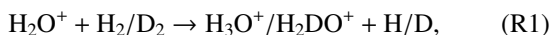
<sup>2</sup>*Department of Chemistry and Chemical Biology, University of New Mexico, Albuquerque, New Mexico 87131, USA*

(Received 9 July 2015; accepted 3 September 2015; published online 18 September 2015)

We have measured the temperature-dependent kinetics for the reactions of  $\text{OH}^+$  with  $\text{H}_2$  and  $\text{D}_2$  using a selected ion flow tube apparatus. Reaction occurs via atom abstraction to result in  $\text{H}_2\text{O}^+/\text{HDO}^+ + \text{H/D}$ . Room temperature rate coefficients are in agreement with prior measurements and resulting temperature dependences are  $T^{0.11}$  for the hydrogen and  $T^{0.25}$  for the deuterated reactions. This work is prompted in part by recent theoretical work that mapped a full-dimensional global potential energy surface of  $\text{H}_3\text{O}^+$  for the  $\text{OH}^+ + \text{H}_2 \rightarrow \text{H} + \text{H}_2\text{O}^+$  reaction [A. Li and H. Guo, *J. Phys. Chem. A* **118**, 11168 (2014)], and reported results of quasi-classical trajectory calculations, which are extended to a wider temperature range and initial rotational state specification here. Our experimental results are in excellent agreement with these calculations which accurately predict the isotope effect in addition to an enhancement of the reaction rate constant due to the molecular rotation of  $\text{OH}^+$ . The title reaction is of high importance to astrophysical models, and the temperature dependence of the rate coefficients determined here should now allow for better understanding of this reaction at temperatures more relevant to the interstellar medium. © 2015 AIP Publishing LLC. [<http://dx.doi.org/10.1063/1.4931109>]

## I. INTRODUCTION

$\text{H}_x\text{O}^+$  type cations (where  $x = 1 - 3$ ) are known to play important roles in interstellar oxygen chemistry<sup>1-3</sup> and have recently been detected in various regions of the interstellar medium (ISM).<sup>4-6</sup> Their formation in the ISM involves several barrierless and highly exoergic reactions. In particular, the following reactions



are among the most important steps in interstellar hydroxyl radical and water formation and, as a consequence, are of high importance to astrophysical models. However, previous kinetic studies have mostly focused on the rate coefficients near room temperature,<sup>7-14</sup> which are less relevant to astrophysical models. The experimental determination of the temperature dependence of rate coefficients for reactions (R1)<sup>15</sup> and (R2) reported in this work found unique behavior which suggests caution when employing room temperature rate coefficients for interstellar models and also provides a better understanding of the role of such molecules in the universe.

These reactions have also served as prototypes for understanding dynamics of ion-molecule reactions in gaseous environments. Ng and coworkers, for example, have found signif-

icant enhancement of reactivity arising from rotational excitation of the reactant ion for reaction (R1) with collision energies up to 10 eV.<sup>16-18</sup> This observation is quite surprising as the reactivity of a typical barrierless complex-forming reaction usually has a weak dependence on reactant internal excitation.<sup>19,20</sup> Theoretical investigations culminating with a full-dimensional *ab initio* potential energy surface (PES) for reaction (R1) have confirmed a barrierless pathway for this exoergic reaction, but they also revealed a bottleneck in the entrance channel in the form of a submerged saddle point, which exerts some control of reaction dynamics with large impact parameters (high  $J$  values).<sup>18,21</sup> Specifically, rotational degrees of freedom of the  $\text{H}_2\text{O}^+$  reactant are strongly coupled with the reaction coordinate at the submerged saddle point.<sup>21</sup> According to the recently proposed Sudden Vector Projection (SVP) model,<sup>22-24</sup> this strong coupling is responsible for the rotational enhancement effect observed by Ng and coworkers. Our recent kinetic measurements of reaction (R1) have yielded rate coefficients from 100 to 600 K, and the agreement with the theoretical results on the new PES was excellent.<sup>15</sup> Interestingly, the rotational effect also manifests itself in the unusual temperature dependence of the rate coefficient, as revealed by our recent work.<sup>15</sup>

Reaction (R2) bears many similarities with reaction (R1). For instance, its PES also has a submerged saddle point in the entrance channel, which is predicted to influence the reaction dynamics.<sup>25</sup> In particular, the rotation of the  $\text{OH}^+$  reactant is predicted by the SVP model to enhance reactivity. Rate coefficients for reaction (R2) have been measured by several authors, but all near 300 K.<sup>13,14</sup> Although the theoretical values

<sup>a)</sup>Present address: College of Chemistry and Materials Science, Northwest University, Xi'an 710069, China.

<sup>b)</sup>Author to whom correspondence should be addressed. Electronic addresses: hguo@unm.edu and afri.rvborgmailbox@kirtland.af.mil.

calculated on the PES are in good agreement with these earlier measurements, little experimental information is known for the temperature dependence, which is vital for modeling the low-temperature oxygen chemistry in the ISM. In this work, we report rate coefficients measured using a variable temperature-selected ion flow tube (VT-SIFT) over a temperature range of 200–600 K. Additionally, the temperature range of the theoretical work was expanded from the original upper limit of 400 K to 600 K to overlap with our new experimental data over the larger temperature range. Agreement between this new set of experimental data and the theoretical work is satisfactory and validates the accuracy of the calculated PES. Observed kinetics are also consistent with an enhanced reactivity, predicted by theory, due to coupling of the OH<sup>+</sup> rotational degree of freedom with the reaction coordinate at the submerged saddle point.

## II. EXPERIMENTAL

Experiments were carried out using a VT-SIFT apparatus which has been extensively described elsewhere.<sup>26–28</sup> Succinctly, ions are created using electron impact ionization on a flow of precursor gases (O<sub>2</sub> and H<sub>2</sub> at ~10–20 std. cm<sup>3</sup> min<sup>−1</sup> each). Ions are extracted from the source region and focused into a mass spectrometer set to select and pass only the relevant ion masses. These ions are subsequently focused and injected into a reaction flow tube via a Venturi inlet. Upon injection, ions are collisionally cooled (ca. 10<sup>4</sup>–10<sup>5</sup> collisions) and entrained by a flow of helium buffer gas (~12 std. l min<sup>−1</sup>; 0.4–1 Torr). A measured flow of neutral reactants (H<sub>2</sub> or D<sub>2</sub>) is introduced into the flow tube at a known distance along its length; primary and product ions are then sampled through a nosecone aperture and focused into a second quadrupole mass spectrometer coupled to an electron multiplier, producing a mass spectrum. Ion intensities are monitored, and rate coefficients are determined by plotting the linear decay of primary ion intensity on a logarithmic scale as a function of neutral reactant flow. Product branching ratios are determined by extrapolating the percent initial product distributions to the initiation of the reaction ([H<sub>2</sub>] = 0). Temperature variability of the reactant rate coefficients and product branching is determined by heating the reaction flow tube (up to ~600 K) using surrounding resistive heaters or cooling (down to ~110 K) using a metered flow of liquid nitrogen through surrounding coiled copper tubing. Overall errors in the rate coefficients are estimated at ±25% absolute and ±15% relative.<sup>26–28</sup>

## III. THEORY

Details of the quasi-classical trajectory (QCT) calculations have been provided in our earlier publication,<sup>25</sup> and only a brief description is given here. All QCT calculations were performed using VENUS.<sup>29</sup> The initial separation of the reactants was 10.0 Å and reactive trajectories are terminated when the separation between the products reaches 7.0 Å. The propagation step was chosen to be 0.02 fs, which was sufficient for energy conservation within the 0.04 kcal mol<sup>−1</sup> cutoff. The forces were obtained by a central differencing method. For a given temperature *T*, both translational and internal degrees of

freedom of the reactants were sampled according to a Boltzmann distribution. The impact parameter was also sampled within a predetermined range. The rate coefficient is calculated based on the following formula:

$$k(T) = \left( \frac{8k_B T}{\pi \mu} \right)^{1/2} \pi b_{\max}^2 \frac{N_r}{N_t}, \quad (1)$$

where  $\mu$  is the translational reduced mass,  $k_B$  is the Boltzmann constant, and  $N_r$  and  $N_t$  are the reactive and total trajectory numbers, respectively. The standard error is given by  $\Delta = \sqrt{(N_t - N_r)/N_t N_r}$ . It is known that classical trajectories may not observe the zero-point energy, but the violation of the product zero-point energy is expected to be minimal due to the large exothermicity of the reaction. The results reported below were obtained with 50 000 trajectories at each temperature with  $b_{\max} = 8.0$  Å, which yielded statistical errors less than 1%. We emphasize that Eq. (1) is only accurate when the rate coefficient depends weakly on the velocity,<sup>30</sup> which is indeed the case here.

Additional reactant rotational-state specified QCT calculations have been performed in order to understand the rotational effect and its influence on the temperature dependence of the rate coefficients. Essentially, the same procedure was used. The corresponding state-specific rate coefficients can be obtained as follows:

$$k_i(T) = \frac{1}{k_B T} \left( \frac{8}{\pi \mu k_B T} \right)^{1/2} \int_0^\infty \sigma_i(E_c) e^{-E_c/k_B T} E_c dE_c, \quad (2)$$

where  $\sigma_i(E_c) = \pi b_{\max}^2(E_c) N_r(E_c)/N_t(E_c)$  is the initial state-specific total integral cross section at the collision energy  $E_c$ . The cross sections have been computed at collision energies up to 1.00 eV. The maximal impact parameter  $b_{\max}$  ranges from 8.0 Å at  $E_c = 0.05$  eV to 4.0 Å at  $E_c = 1.00$  eV. The standard error of these cross sections is typically around 2% with 30 000 trajectories at each  $E_c$ .

Reaction (R2) proceeds on the lowest triplet state of H<sub>3</sub>O<sup>+</sup>. Given the lightness of the atoms involved, intersystem crossing to the ground singlet state ( $\tilde{X}^1A$ ) PES is unlikely. The  $\tilde{a}^3A$  state PES used in the QCT calculations was developed from ~30 000 Davidson corrected multi-reference configuration interaction points with the aug-cc-pVTZ basis set.<sup>25</sup> The fit has a root-mean square error of 3.0 meV, thanks to the high-fidelity permutation-invariant polynomial-neural network method.<sup>31,32</sup> The long-range interaction in the entrance channel has been modeled using an analytic form but confirmed by high-level *ab initio* data. For more details of the PES, the reader is referred to our recent publication.<sup>25</sup>

## IV. RESULTS AND DISCUSSION

In Figure 1, the PES along the reaction pathway for reaction (R2) is shown with geometries of important points along the MEP. It should be noted that the reactant asymptote is at energy zero and the point A corresponds to the pre-reaction well formed between the two reactants. With that in mind, it is clear that the saddle point B is submerged but is high enough so that it can rise above the reactant asymptote with a large centrifugal potential due to the overall rotation of the

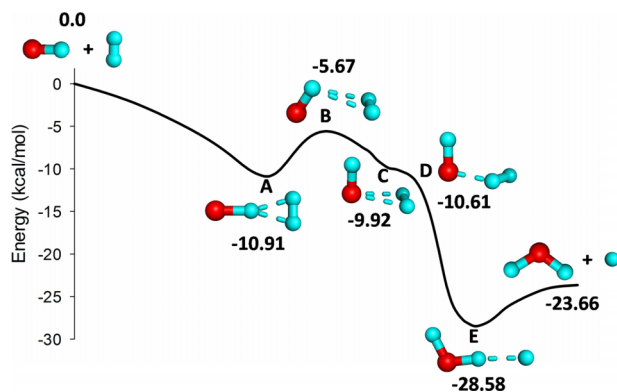


FIG. 1. Schematic pathway on the PES for reaction (R2) along with associated geometries. Zero energy is chosen at the reactant asymptote.

reactive system. This feature is similar to the PES for reaction (R1) and may endow the rate coefficient with a complicated temperature dependence. Beyond this submerged saddle point, there are a few other structures that might influence the reaction dynamics before the product complex (point E) is formed. This product complex is very shallow towards the formation of the  $\text{H}_2\text{O}^+ + \text{H}$  product channel, and as a result, is not expected to have a significant lifetime. Consequently, H-D exchange in this well is unlikely.

At room temperature, the experimental rate coefficients of reaction (R2) are  $1.1 (\pm 0.3) \times 10^{-9} \text{ cm}^3 \text{ molecule}^{-1} \text{ s}^{-1}$  and  $7.5 (\pm 1.9) \times 10^{-10} \text{ cm}^3 \text{ molecule}^{-1} \text{ s}^{-1}$  for  $\text{H}_2$  and  $\text{D}_2$ , respectively. The room temperature value for the  $\text{H}_2$  reaction agrees well with the prior experimental values of  $8.6 (\pm 2.6) \times 10^{-10} \text{ cm}^3 \text{ molecule}^{-1} \text{ s}^{-1}$  and  $1.01 (\pm 0.20) \times 10^{-9} \text{ cm}^3 \text{ molecule}^{-1} \text{ s}^{-1}$  determined by Shul *et al.* and Jones *et al.*, respectively.<sup>13,14</sup> Our values throughout the 200–600 K temperature range are given with efficiencies in Table I. The simple Langevin collision rate constant employed here is equivalent to the parameterization of Su-Chesnavich<sup>33</sup> when no permanent dipole is present, and varies minimally from detailed methodologies, such as that by Ervin<sup>34</sup> including anisotropic polarizabilities and quadrupole moments, over this temperature range. Values for efficiency are slightly over 50% at the lowest temperature (200 K) and grow with increasing temperature, somewhat more so for reaction with  $\text{D}_2$  than with  $\text{H}_2$ .

Reaction rate coefficients are also plotted in Figure 2 alongside results from the QCT theoretical work. The data are in good agreement and follow similar temperature dependences. Agreement between experiment and theory throughout the temperature range confirms the validity of the PES. As

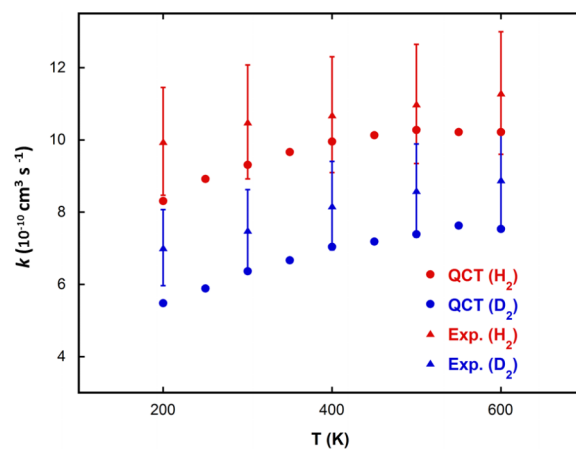


FIG. 2. Comparison of experimental and theoretical results for the temperature dependence of rate coefficients for the  $\text{OH}^+ + \text{H}_2/\text{D}_2$  reaction. Error bars represent 15% relative error.

seen from the data, experimental values for both  $\text{H}_2$  and  $\text{D}_2$  were consistently higher. This discrepancy is larger than that for reaction (R1)<sup>15</sup> and is presumably due to remaining errors in the PES or in the QCT approximation of the reactive scattering. Reaction of  $\text{OH}^+$  with both  $\text{H}_2$  and  $\text{D}_2$  displays a weak positive temperature dependence,  $T^{0.11}$  for the normal and  $T^{0.25}$  for the deuterated reactions.

Unlike reaction (R1), our data do not show a maximum in the temperature dependence for reaction (R2) within the temperature range studied here. As discussed in our earlier work,<sup>15</sup> the unusual temperature dependence for the rate coefficient of reaction (R1) was attributed to the rotational enhancement effect discovered by Ng and coworkers.<sup>16–18</sup> To shed light on the rotational effects in reaction (R2), Figure 3 shows the calculated initial rotational state specific rate coefficients for both  $\text{H}_2$  and  $\text{OH}^+$  as a function of translational temperature. It is clear from the figure that the rate coefficient for the ground rotational states of both reactants already has a positive translational temperature dependence. However, rotational excitation of both reactions does increase the reactivity substantially with a larger effect for  $\text{OH}^+$  than for  $\text{H}_2$  even though the excitation energy of the latter is larger. Thus, the positive temperature effect has contributions from both rotational and translational energies. This enhancement is consistent with the prediction by the SVP model that the  $\text{OH}^+$  rotational mode is coupled with the reaction coordinate at the submerged saddle point.<sup>25</sup>

The kinetic isotope effect (KIE) for  $\text{H}_2$  and  $\text{D}_2$  is displayed in Figure 4, in which the  $\text{D}_2$  apparently reacts with

TABLE I. Experimental rate coefficients and efficiencies.

Temperature (K)	$\text{OH}^+ + \text{H}_2$		$\text{OH}^+ + \text{D}_2$	
	$k$ ( $10^{-10} \text{ cm}^3 \text{ s}^{-1}$ )	$k/k_{\text{Langevin}}^a$	$k$ ( $10^{-10} \text{ cm}^3 \text{ s}^{-1}$ )	$k/k_{\text{Langevin}}$
200	10.3	0.63	6.8	0.59
300	10.5	0.67	7.5	0.64
400	10.7	0.68	8.2	0.71
500	11.0	0.70	8.6	0.74
600	11.3	0.72	8.9	0.77

$$^a k_{\text{Langevin}} = 2\pi q \sqrt{\frac{\alpha}{\mu}}$$



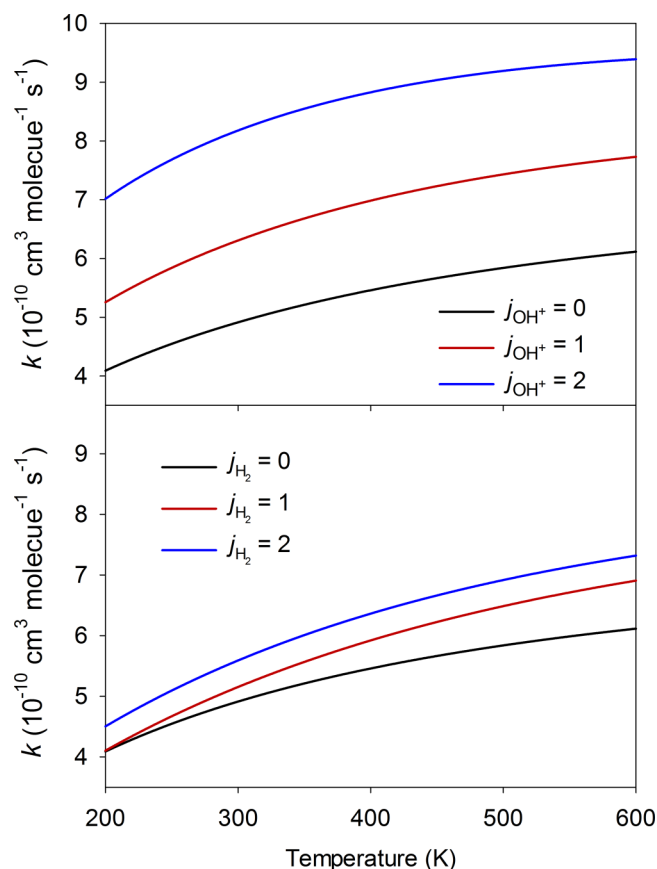


FIG. 3. Calculated initial state-specific rate coefficients for reaction (R2) as a function of translational temperature. Top panel: rate coefficients for three rotational states of  $\text{OH}^+$  with rotationless  $\text{H}_2$ ; bottom panel: rate coefficients for three rotational states of  $\text{H}_2$  with rotationless  $\text{OH}^+$ .

a smaller rate coefficient at all temperatures. A similar KIE was observed for reaction (R1). Also evident in the figure is the exceptional accord in KIE between experiment and theory. The experiment-theory agreement of KIE for reaction (R2) is much better than that for reaction (R1).<sup>21</sup> As discussed by Li and Guo, the KIE observed for reaction (R2) is similar to that observed in the earlier joint experimental/theoretical work

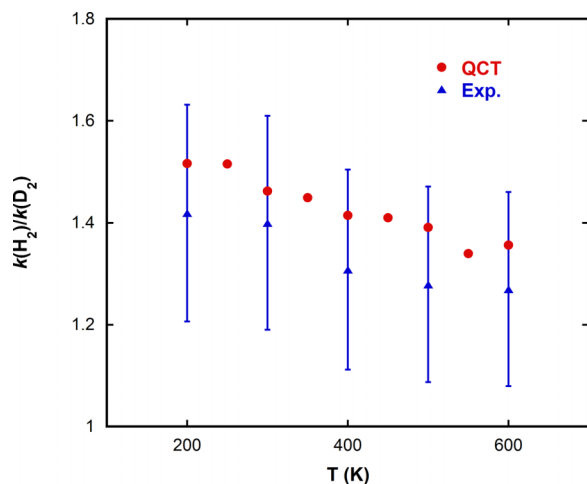


FIG. 4. Comparison of experimental and calculated kinetic isotope effects for the  $\text{OH}^+ + \text{H}_2/\text{D}_2$  reaction. Error bars represent 15% relative error.

on reaction (R1)<sup>15</sup> and is likely due to the smaller zero-point energy associated with  $\text{D}_2$ .<sup>21,25</sup> While the majority of the KIE is a function of the collision rate difference, as the reactions are of similar efficiencies, the modelling of the subtle temperature dependence of the KIE is particularly impressive.

Theoretically, the reaction between  $\text{OH}^+$  and  $\text{D}_2$  could produce both  $\text{HOD}^+$  and  $\text{D}_2\text{O}^+$  products. We scrutinized these two product channels and saw no evidence of the  $\text{D}_2\text{O}^+$  product. We tentatively set an upper limit of 5% for this channel. This observation is consistent with our trajectory results, in which the  $\text{HOD}^+$  product also dominates (at 300 K, only 3 out of 50 000 trajectories produce  $\text{D}_2\text{O}^+$ ). The dominance of the  $\text{HOD}^+$  product also reflects the reaction pathway depicted in Figure 1, in which the reactivity is largely controlled by the entrance channel, particularly by the submerged barrier. Once the system passes the bottleneck, dissociation into products is rapid and direct.

The lack of scrambling along the reaction path and the observed positive temperature dependence of the reaction rate deserve comment since they suggest implications for the theoretical treatment of this system. While previous work on reaction (R1)<sup>15</sup> rationalized the observed complicated temperature dependence as a combination of rotational enhancement with a negative translational energy dependence which is typical of statistically behaved reactions that are inhibited by a submerged barrier, that interpretation is insufficient for the present case. Each of the calculated rotational levels displayed a positive translational temperature dependence. A statistically behaved system, i.e., one with a long-lived intermediate complex, would display a flat or negative translational temperature dependence when inhibited by a submerged barrier such as the one shown in Fig. 1.<sup>35</sup> The calculated positive translational temperature dependence for each individual rotational state along with the lack of scrambling shows that the reaction does not proceed statistically. Furthermore, the depth of the pre-reaction intermediate complex (stationary point A) is sufficiently small to be consistent with non-statistical behavior, i.e., the lifetime in the well is extremely short. Trajectory calculations, such as those employed here, are therefore vital towards understanding the reactivity of such systems and extending modelling towards experimentally inaccessible regimes.

Unfortunately, neither the experimental nor computational methods used here can reliably determine the rate coefficients at astrophysically relevant temperatures of 10–50 K. The QCT calculations used here ignore quantum effects, such as tunneling, that could become significant at such low temperatures. Because the nature of the temperature dependence is not entirely understood, a simple extrapolation of the present results is unwise. However, noting the dependence of the rate coefficient on the rotational energy of the  $\text{OH}^+$  and the dominance of the  $j = 0$  state at low temperatures, the thermally averaged 300 K rate coefficient of  $\sim 10^{-9} \text{ cm}^3 \text{ s}^{-1}$  for reaction (R2), as employed in kinetic modeling of the interstellar medium,<sup>3</sup> appears too large a value. The  $j = 0$  rate constant at 200 K is roughly  $4 \times 10^{-10} \text{ cm}^3 \text{ s}^{-1}$  and decreases with lower temperature. Therefore, we suggest this as an upper limit to what should be used in astrochemical models.

## V. SUMMARY

Ion-molecule reactions often feature barrierless pathways and long-lived intermediates. As a result, the rate coefficients often have weak or null temperature dependence. Kinetics of such reactions can often be explained by statistical theory.<sup>36,37</sup> Recently, however, it has become possible to move beyond the statistical picture and examine dynamical issues in ion-molecule reactions, as demonstrated by recent work on  $S_N2$  reactions.<sup>38,39</sup> The dynamical approach involves the development of accurate global PESs from high-level *ab initio* calculations over a large configuration space, followed by either quasi-classical trajectory or quantum wave packet studies on the PESs. These studies are starting to reveal important dynamical features in ion-molecule reactions, and they might also manifest in the temperature dependence of the rate coefficients, as demonstrated recently by us for reaction (R1).<sup>15</sup>

In conclusion, we have measured the rate coefficients for the reaction of  $OH^+$  with both  $H_2$  and  $D_2$  from 200 K to 600 K. Furthermore, we have extended predictions from a QCT method on an accurate PES over this temperature range for comparison. Results indicate agreement between experiment and theory, suggesting that the calculated PES for the reaction is qualitatively correct. The experimental isotope effect is predicted by theory extremely well, including the temperature dependence. We have also examined the influence of reactant rotational excitations and found that the  $OH^+$  rotation strongly enhances the reactivity, in accord with the prediction by the SVP model. On the other hand, the rotational excitation of the  $H_2$  reactant has a relatively small effect especially considering the relative energies of the rotational excitations. While the QCT method employed is not reliable at astrochemically relevant temperatures for this system, it is clear from the observed temperature dependence and the predicted rotational enhancement that the rate coefficient for this system is likely to be significantly smaller than that at room temperature. As such a lower value of  $4 \times 10^{-10} \text{ cm}^3 \text{ s}^{-1}$ , corresponding to the  $j = 0$  rate constant at 200 K, is suggested only as an upper limit to values which should be incorporated within astrophysical models.

## ACKNOWLEDGMENTS

Support for this work comes from the following sources: H.G.—the Air Force Office of Scientific Research (Grant No. AFOSR-FA9550-15-1-0305) and A.A.V.—the Air Force Office of Scientific Research (Grant No. AFOSR-2303EP). O.M. acknowledges support from the National Research Council and S.G.A. acknowledges support from the Boston College Institute of Scientific Research. A.L. acknowledges partial support from the Scientific Foundation of Northwest University (Grant No. 338050068).

<sup>1</sup>E. Herbst and W. Klemperer, *Astrophys. J.* **185**, 505 (1973).

<sup>2</sup>W. D. Watson, *Acc. Chem. Res.* **10**, 221 (1977).

<sup>3</sup>D. Hollenbach, M. J. Kaufman, D. Neufeld, M. Wolfire, and J. R. Goicoechea, *Astrophys. J.* **754**, 105 (2012).

<sup>4</sup>D. A. Neufeld, J. R. Goicoechea, P. Sonnentrucker, J. H. Black, J. Pearson, S. Yu, T. G. Phillips, D. C. Lis, M. De Luca, E. Herbst, P. Rimmer, M. Gerin, T. A. Bell, F. Boulanger, J. Cernicharo, A. Coutens, E. Dartois, M. Kazmierczak, P. Encarnaz, E. Falgarone, T. R. Geballe, T. Giesen, B. Godard, P. F. Goldsmith, C. Gry, H. Gupta, P. Hennebelle, P. Hily-Blant, C. Joblin, R. Kolos, J. Krelowski, J. Martin-Pintado, K. M. Menten, R. Monje, B. Mookerjee, M. Perault, C. Persson, R. Plume, M. Salez, S. Schlemmer, M. Schmidt, J. Stutzki, D. Teyssier, C. Vastel, A. Cros, K. Klein, A. Lorenzani, S. Philipp, A. Samoska, R. Shipman, A. G. G. M. Tielens, R. Szczerba, and J. Zmuidzinas, *Astron. Astrophys.* **521**, L10 (2010).

<sup>5</sup>M. Gerin, M. De Luca, J. Black, J. R. Goicoechea, E. Herbst, D. A. Neufeld, E. Falgarone, B. Godard, J. C. Pearson, D. C. Lis, T. G. Phillips, T. A. Bell, P. Sonnentrucker, F. Boulanger, J. Cernicharo, A. Coutens, E. Dartois, P. Encarnaz, T. Giesen, P. F. Goldsmith, H. Gupta, C. Gry, P. Hennebelle, P. Hily-Blant, C. Joblin, M. Kazmierczak, R. Kolos, J. Krelowski, J. Martin-Pintado, R. Monje, B. Mookerjee, M. Perault, C. Persson, R. Plume, P. B. Rimmer, M. Salez, M. Schmidt, J. Stutzki, D. Teyssier, C. Vastel, S. Yu, A. Contursi, K. Menten, T. Geballe, S. Schlemmer, R. Shipman, A. Tielens, S. Philipp-May, A. Cros, J. Zmuidzinas, L. A. Samoska, K. Klein, and A. Lorenzani, *Astron. Astrophys.* **518**, L110 (2010).

<sup>6</sup>E. Gonzalez-Alfonso, J. Fischer, S. Bruderer, H. S. P. Muller, J. Gracia-Carpio, E. Sturm, D. Lutz, A. Poglitsch, H. Feuchtgruber, S. Veilleux, A. Contursi, A. Sternberg, S. Hailey-Dunsheath, A. Verma, N. Christopher, R. Davies, R. Genzel, and L. Tacconi, *Astron. Astrophys.* **550**, A25 (2013).

<sup>7</sup>D. A. Kubose and W. H. Hamill, *J. Am. Chem. Soc.* **85**, 125 (1963).

<sup>8</sup>F. C. Fehsenfeld, A. L. Schmeltekopf, and E. E. Ferguson, *J. Chem. Phys.* **46**, 2802 (1967).

<sup>9</sup>A. G. Harrison and J. C. J. Thynne, *Trans. Faraday Soc.* **64**, 945 (1968).

<sup>10</sup>J. K. Kim, L. P. Theard, and W. T. Huntress, *J. Chem. Phys.* **62**, 45 (1975).

<sup>11</sup>I. Dotan, W. Lindinger, B. Rowe, D. W. Fahey, F. C. Fehsenfeld, and D. L. Albritton, *Chem. Phys. Lett.* **72**, 67 (1980).

<sup>12</sup>A. B. Rakshit and P. Warneck, *J. Chem. Phys.* **74**, 2853 (1981).

<sup>13</sup>J. D. C. Jones, K. Birkinshaw, and N. D. Twiddy, *Chem. Phys. Lett.* **77**, 484 (1981).

<sup>14</sup>R. J. Shul, R. Passarella, L. T. Difazio, R. G. Keese, and A. W. Castleman, *J. Phys. Chem.* **92**, 4947 (1988).

<sup>15</sup>S. G. Ard, A. Li, O. Martinez, N. S. Shuman, A. A. Viggiano, and H. Guo, *J. Phys. Chem. A* **118**, 11485 (2014).

<sup>16</sup>Y. Xu, B. Xiong, Y. C. Chang, and C. Y. Ng, *J. Chem. Phys.* **137**, 241101 (2012).

<sup>17</sup>Y. Xu, B. Xiong, Y. C. Chang, and C. Y. Ng, *J. Chem. Phys.* **139**, 024203 (2013).

<sup>18</sup>A. Li, Y. Li, H. Guo, K.-C. Lau, Y. Xu, B. Xiong, Y.-C. Chang, and C. Y. Ng, *J. Chem. Phys.* **140**, 011102 (2014).

<sup>19</sup>J. Troe, *J. Chem. Soc., Faraday Trans.* **90**, 2303 (1994).

<sup>20</sup>H. Guo, *Int. Rev. Phys. Chem.* **31**, 1 (2012).

<sup>21</sup>A. Li and H. Guo, *J. Chem. Phys.* **140**, 224313 (2014).

<sup>22</sup>B. Jiang and H. Guo, *J. Chem. Phys.* **138**, 234104 (2013).

<sup>23</sup>B. Jiang and H. Guo, *J. Am. Chem. Soc.* **135**, 15251 (2013).

<sup>24</sup>H. Guo and B. Jiang, *Acc. Chem. Res.* **47**, 3679 (2014).

<sup>25</sup>A. Li and H. Guo, *J. Phys. Chem. A* **118**, 11168 (2014).

<sup>26</sup>J. C. Poutsma, A. J. Midey, and A. A. Viggiano, *J. Chem. Phys.* **124**, 4 (2006).

<sup>27</sup>A. A. Viggiano, R. A. Morris, F. Dale, J. F. Paulson, K. Giles, D. Smith, and T. Su, *J. Chem. Phys.* **93**, 1149 (1990).

<sup>28</sup>A. A. Viggiano and R. A. Morris, *J. Phys. Chem.* **100**, 19227 (1996).

<sup>29</sup>X. Hu, W. L. Hase, and T. Pirraglia, *J. Comput. Chem.* **12**, 1014 (1991).

<sup>30</sup>K. N. Swamy and W. L. Hase, *J. Am. Chem. Soc.* **106**, 4071 (1984).

<sup>31</sup>B. Jiang and H. Guo, *J. Chem. Phys.* **139**, 054112 (2013).

<sup>32</sup>J. Li, B. Jiang, and H. Guo, *J. Chem. Phys.* **139**, 204103 (2013).

<sup>33</sup>T. Su and W. J. Chesnavich, *J. Chem. Phys.* **76**, 5183 (1982).

<sup>34</sup>K. M. Ervin, *J. Int. Mass Spectrom.* **378**, 48 (2015).

<sup>35</sup>J. Troe, *J. Int. Mass Spectrom. Ion Phys.* **80**, 17 (1987).

<sup>36</sup>M. Quack and J. Troe, *Ber. Bunsen-Ges. Phys. Chem.* **78**, 240 (1974).

<sup>37</sup>T. Baer and W. L. Hase, *Unimolecular Reaction Dynamics, Theory and Experiments* (Oxford University Press, New York, 1996).

<sup>38</sup>J. Mikosch, S. Trippel, C. Einhorn, R. Otto, U. Lourderaj, J. X. Zhang, W. L. Hase, M. Weidmuller, and R. Wester, *Science* **319**, 183 (2008).

<sup>39</sup>P. Manikandan, J. Zhang, and W. L. Hase, *J. Phys. Chem. A* **116**, 3061 (2012).